RESEARCH PAPER

Synthesis and *in vitro* characterization of PCL-PEG-HA/FeCo magnetic nanoparticles encapsulating curcumin and 5-FU

Shima Bourang [1], Mehran Noruzpour [1], Solmaz Azizi [1], Hashem Yaghoubi [2]*, Hossein Ali Ebrahimi [3]

[1]Department of Agronomy and Plant Breeding, Faculty of Agriculture and Natural Resources, University of Mohaghegh Ardabili, Ardabil, Iran
[2]Department of Biology, Ardabil Branch, Islamic Azad University, Ardabil, Iran
[3]Department of Pharmaceutics, School of Pharmacy, Ardabil University of Medical Sciences, Ardabil, Iran

ABSTRACT

Objective(s): Colorectal cancer is the second deadly cancer for men and women worldwide. Depending on the pathological attributes of the tumor, there are numerous therapeutic options for colorectal cancer treatment. Chemotherapy is one of the main methods, however, due to the low solubility and short half-life of chemotherapy drugs, this treatment method has limitations. 5-Fu and curcumin are important drugs for the treatment of colorectal cancer. One of the primary resolutions is the application of bioanalytical techniques, which involve the utilization of chemotherapy agents in conjunction with nanoparticles, thereby facilitating the directed transportation of the therapeutic substance to malignant cells.

Materials and Methods: In this study, Polycaprolactone- Polyethylene glycol- Hyaluronic acid (PCL-PEG-HA) copolymers and magnetic nanoparticle iron-cobalt (FeCo) were synthesized to deliver Curcumin (CU), 5-Fluorouracil (5-Fu) and the combination to HCT116 colorectal cancer cells. To control the release of CU and 5-FU and *in vivo* tumor targeting, PCL-PEG-HA/FeCo were synthesized and then characterized for the morphological characteristics, shape, and magnetic properties of the nanoparticles, drug retention efficiency, and release pattern in two acidic and neutral environments.

Results: Our results demonstrated that the release profile of CU and 5-FU from the nanoparticles in acidic conditions was more than the drug release in neutral conditions. In acidic conditions, due to faster degradation of nanoparticles, drugs are released faster. Moreover, these nanoparticles have high biocompatibility and potential in transporting CU and 5-FU drugs to HCT116 cells. The IC_{50} of co-delivery of CU and 5-FU was 65.42 mg/L, while, the IC_{50} value of drugs coated with nanoparticles (PCL-PEG-HA/FeCo/5-FU/Curcumin) was 72.26. Otherwise, utilizing nanoparticles can increase the amount of apoptosis compared to control and free 5-Fu and Curcumin.

Conclusion: In conclusion, PCL-PEG-HA/FeCo/5-FU/Curcumin nanoparticles can be an efficient solution in targeted drug delivery to colorectal cancer cells and reducing the side effects of these drugs on normal cells.

Keywords: Chemotherapy drugs, Drug delivery, Hyaluronic acid, Polycaprolactone, Polyethylene glycol

INTRODUCTION

Colorectal cancer (CRC) is the third most common diagnosis and second deadliest malignancy for both sexes combined [1]. In the year 2020, it is predicted that CRC will account for 1.9 million cases and 0.9 million deaths worldwide [2]. In recent times, there has been a significant increase in scientific research on the comprehensive management of colorectal cancer. Moreover, the primary therapeutic approach for patients suffering from metastatic colorectal cancer (mCRC) involves a combination regimen that incorporates the use of a specifically targeted medication [2]. Despite the progression of drug regimens in CRC, it is difficult to achieve treatment of mCRC because of the poor prognosis with a median overall survival (mOS) of only 25-30 months [3, 4]. Different treatment procedures are available for CRC, for patients with metastatic colorectal cancer, the primary therapeutic approach is palliative chemotherapy, while non-

systematic treatments such as surgery, optional radiation, and ablative techniques are considered for patients with resectable metastatic lesions in order to enhance overall survival. Neoadjuvant and palliative chemotherapy [5], immunotherapy [6], and tyrosine kinase inhibitor (TKI) therapy [7] are other CRC treatments. Currently, targeted drug delivery by nanoparticles is a new approach to solve various problems related to chemotherapeutic drugs [8].

One of the frequently utilized antimetabolite agents in the primary therapeutic approach for colorectal cancer is 5-fluorouracil (5-FU), an aqueous anti-neoplastic medication used to treat pancreatic, gastric, and breast malignancies [9, 10]. The active derivatives of 5-FU have the capability to interfere with both the synthesis of DNA and RNA, impede the proliferation of cancer cells, and initiate a process called apoptosis. 5-FU is a derivative of uracil and possesses a fluorine atom in place of hydrogen at the C-5 position. Upon entering the cell, 5-FU is converted to various metabolites that are active biologically, such as fluorodeoxyuridine monophosphate (FdUMP), fluorodeoxyuridine triphosphate (FdUTP), and fluorouridine triphosphate (FUTP). These metabolites provide important roles in disrupting RNA synthesis and also exhibit anti-cancer effects by inhibiting the enzyme thymidylate synthase (TS) [10]. Active metabolites of 5-FU disrupt both DNA and RNA synthesis, block cancer cell proliferation and induce apoptosis [11]. In CRC, the administration of intravenous and oral 5-FU or other fluoropyrimidines (FPs) has emerged as the primary approach to systemic therapy since the 1990s. Since that time, researchers have concentrated on the biomodulation of 5-FU to improve its therapeutic effectiveness and cytotoxicity [12]. Co-administration of 5-FU in company with natural or synthetic drugs like doxorubicin [13], paclitaxel/cisplatin [14, 15], curcumin [9, 16], metformin [17, 18], irinotecan/oxaliplatin [19] demonstrated development in response rates and medicinal results.

Curcumin, a prominent chromatic compound obtained from the subterranean stem of the botanical species Curcuma longa, belonging to the family Zingiberaceae, is widely recognized under the name of turmeric [20]. Curcumin has different effects, including anti-oxidant, anti-inflammatory, anti-bacterial, hepatoprotective, anti-viral, and anti-diabetic properties. Consequently, it has been widely investigated

for its anti-cancer activity across multiple cancer types, including CRC [21, 22]. Whereas it shows the inhibitory impacts on CRC cells *in vitro* [23], the pharmacokinetic data revealed its poor aqueous solubility, low oral absorption, and low bioavailability. Thus, it has not been sufficiently effective in animal models and clinical trials [24]. However, in recent years, many curcumin preparations using technology to increase its aqueous solubility, stability, absorption, and bioavailability have been developed [25]. When Curcumin is co-administered with other anticancer drugs, it enhances the cytotoxicity of these synergistic agents, thereby making it a promising candidate for combination therapy. The co-administration of Curcumin and 5-FU enhances the chemosensitivity of the initial chemotherapeutic agent (5-FU) for colorectal cancer via the modulation of Src, NF-kB, and NF-NB-dependent regulated gene products. Upon examination in a high-density culture, Curcumin, whether used alone or in combination with 5-FU, effectively inhibits colonoscopy formation, induces apoptosis, suppresses proliferation, and downregulates colon cancer cell markers in MMR-deficient 5-FU-resistant cells [26].

Bioanalytical techniques and biomedical applications are entirely dependent on the utilization of magnetic nanoparticles [27]. When dealing with biological specimens, these methods experience reduced levels of background interference, resulting in the magnetic susceptibilities of bio-type samples being virtually non-existent [28]. Examples of biomedical applications that can now be implemented using magnetic nanoparticles include analytical tools, bioimaging, biosensors, contrast agents (CAs), hyperthermia, photoablation therapy, physical therapy applications, separation, signal markers, and targeted drug delivery (TDD). The specific targeting of magnetic nanoparticles reduces the adverse effects of the drug as it prevents non-specific uptake into normal cells. Conversely, increasing the drug dosage in the affected area enhances its efficacy compared to free drug employment. Due to their strong magnetic properties and other characteristics such as temperature sensitivity and exceptional biocompatibility, these nanoparticles have attracted considerable attention among many researchers in recent times [29]. Among various types of magnetic nanoparticles, FeCo-(Iron,

Cobalt)$_3$O$_4$ nanoparticles demonstrate superior magnetic saturation with a value of 215 emu/g, in comparison to other magnetic materials such as Fe$_3$O$_4$ (21–80 emu/g), Fe$_5$C$_2$ (125 emu/g), and PtFe (100 emu/g) nanoparticles. FeCo-(Fe,Co)$_3$O$_4$ nanoparticles containing ferromagnetic iron (Fe) and cobalt (Co) as well as their alloys and oxides have been proven to be the most promising probes for theranostics and targeted drug delivery systems. However, they possess a pronounced inclination towards agglomeration, which refers to the phenomenon where the particles of a substance adhere together under specific conditions, resulting in the formation of a cohesive mass of that particular material. Moreover, FeCo nanoparticles are also susceptible to oxidation. To solve the issues of agglomeration, oxidation, and toxicity, the surfaces of magnetic nanoparticles are coated with natural hydrophilic polymers such as starch, cellulose, chitin, chitosan, gelatin, and others [30].

The degradation of Polycaprolactone (PCL) occurs via the hydrolysis of its ester linkages in physiological environments and in the human body. Consequently, PCL has garnered significant interest as a biomaterial suitable for implantation and controlled drug release scenarios [31]. However, in the field of tissue engineering, PCL faces certain drawbacks such as a slow degradation rate, lower mechanical properties, and limited cell adhesion. In order to overcome these limitations, PCL can undergo polymerization with other polymers such as Polyethylene glycol (PEG), Polylactic acid (PLA), Hyaluronic acid (HA), Polyglycolide or poly (glycolic acid) (PGA), and so on [32]. PEG is a synthetic, hydrophilic polyether compound that is both biocompatible and biodegradable and finds extensive applications primarily within the medical industry, but also in the chemical and industrial sections. Similar to PCL, PEGs have been approved by the Food and Drug Administration (FDA) as exceptional materials for many biomedical applications due to their biodegradability and biocompatibility [33, 34]. HA, a fundamental constituent of the extracellular matrix, is employed due to its compatibility with living organisms, ability to degrade naturally, lack of toxicity, and absence of immunogenicity. Additionally, this acid provides many locations for modification, such as carboxyl and hydroxyl groups, which are commonly utilized for the delivery of antineoplastic agents [35].

The objective of this study is to utilize FeCo nanoparticles coated with a copolymer of PCL-PEG-HA in order to create a targeted nanocarrier for 5-Flourouracil and Curcumin. The efficiency of 5 Fu, Curcumin (CU), and their combination was examined in this investigation. Subsequently, the physicochemical properties, drug release pattern, toxicity, and efficacy of PCL-PEG-HA/FeCo/5-FU, PCL-PEG-HA/FeCo/CU, and PCL-PEG-HA/5-FU/CU nanoparticles were assessed in terms of drug delivery on the colorectal cancer cell line HCT116.

MATERIALS AND METHODS
Materials

For this research, Polyvinyl alcohol (PVA), Chloroform (CHCl$_3$), NHS (N-Hydroxysuccinimid), and Oleic acid were purchased from Merck. Hyaluronic acid (HA), RPMI Media, MTT assay Kit, DMSO (Dimethyl sulfoxide), PCL-COOH (poly ε-caprolactone), EDC (N-Ethyl-N′-(3-dimethylaminopropyl)-carbodiimid -hydrochlorid), PEG (poly ethylene glycol), Curcumin, FeCo, PBS (Phosphate buffered saline), and FBS (Fetal Bovine Serum) were purchased from Sigma Aldrich company and 5-Fluorouracil was acquired from Ebewe pharma company.

Synthesis of PCL-PEG-HA copolymer

To polymerize PCL-PEG-HA, first, the Carboxylic acid group of PCL-COOH polymer was activated by adding 100 mg of NHS and 200 mg of EDC to 1 g of PCL-COOH solutions in 20 ml chloroform and was kept at room temperature for one hour. Second, to conduct a reaction between PCL-COOH and NH$_2$-PEG-HA, 2 g of NH$_2$-PEG-HA was added to PCL-COOH solution and mixed slowly for 2 days of stirring at room temperature. Finally, to remove impurities, the resulting product was centrifuged for half an hour at 4 °C (15000 rpm) using equal volumes of water and methanol. The copolymer was further purified using dialysis membranes (10000 MW) and then the PCL-PEG-HA polymer was centrifuged again under the above-mentioned conditions and freeze-dried.

Characterization of PCL-PEG-HA copolymer

H-NMR spectroscopy was carried out to investigate the structure of PCL-PEG-HA copolymer using CDCl$_3$ as the solvent (Varian Unityinova 500 NMR Spectrometer, USA). Additionally, the FTIR technique (1B-AR-010, Biotec, USA) was used to

confirm the synthesis of PCL-PEG-HA synthesis. Also, the thermal stability of PCL and PCL-PEG-HA copolymer was evaluated by Thermogravimetric analysis (TGA, STA-PT1000, License, Germany) in a thermal range of 40 °C to 700 °C with a heating rate of 10 °C/min.

Synthesis of PCL-PEG-HA/FeCo/5-FU/Curcumin, PCL-PEG-HA/FeCo/5-FU, PCL-PEG-HA/FeCo/ Curcumin and PCL-PEG-HA/ FeCo nanoparticles

A solvent diffusion technique was used to prepare PCL-PEG-HA/FeCo/5-FU/Curcumin. For this purpose, 5 mg of FeCo nanoparticle coated with Oleic Acid were added to separate PCL-PEG-HA solutions (30 mg in 1 ml chloroform). Then, 4 mg of 5-FU and 4 mg of Curcumin were added to the mixture and sonicated for 30 seconds, and then 1 ml of PVA solutions (1% w/v) were added to the mixture and sonicated for another 30 sec, respectively. The resulting emulsions were then collected using a syringe and slowly injected into 25 ml of PVA solution (0.3% w/v) under stirring. The final emulsion was stirred at room temperature for 24 hr. The yielded nanoparticles were washed 3 times with centrifugation using deionized water (13000 rpm for 1 hr) and freeze-dried.

As well asBesides, to prepare PCL-PEG-HA/FeCo nanoparticles (without drug) and PCL-PEG-HA/FeCo/5-FU and PCL-PEG-HA/FeCo/Curcumin nanoparticles, the above technique was used. With the difference that only drug 5-FU or Curcumin was used in the loading stages. Also, in order to prepare PCL-PEG-HA/FeCo nanoparticles, loading steps without 5-FU and Curcumin drugs were carried out.

Characterization of nanoparticles

The average size and zeta potential of the synthesized nanoparticles were determined using dynamic light scattering (DLS, SZ100, Horiba, Japan) techniques. The morphology and size distribution of nanoparticles were investigated by TEM images (LEO906, Zeiss, Germany). The formation of magnetite nanoparticles was confirmed by FTIR and UV-Vis (Thermo Scientific, USA) spectroscopy. VSM (Vibrating Sample Magnetometer, MDKF-Co., Iran) technique was used to measure the magnetic properties of FeCo nanoparticles. The particle size and zeta potential were measured by dynamic light scattering (DLS) (Malvern Instruments, Westborough, MA, USA). Polydispersity Index (PdI) is was used to estimate the average uniformity of a particle solution, and larger PdI values correspond to a larger size distribution in the particle sample. PdI can also indicate nanoparticle aggregation along with the consistency and efficiency of particle surface modifications throughout the particle sample.

Determination of drug encapsulation efficiency of synthesized nanoparticles

To calculate the encapsulation efficiency of drug 5-FU, and Curcumin encapsulation efficiency ofin PCL-PEG-HA/FeCo/5-FU/CU, PCL-PEG-HA/FeCo/5-FU and PCL-PEG-HA/FeCo/CU nanoparticles, the supernatant of the nanoparticle's mixture was centrifuged (13000 rpm for 1 hr) and the amount of free 5-FU and Curcumin present in the supernatant was determined using spectrophotometry at 260 nm (5-FU) and 480 nm (Curcumin). The measured amount was then compared with the initial amount of drug used in the loading process (4 mg of each drug) and the encapsulation efficiency was calculated by the following equation (Equation 1-1):

EE%= (Winitial 5-FU or CU − Wfree 5-FU or CU / Winitial 5-FU or CU)

Release profile of drug from nanoparticles

Since the tumor tissue has a lower pH compared to the normal tissue, the drug release from nanoparticles was evaluated in PBS buffer with acidic (pH = 6) and neutral (pH = 7.4) pH values. 10 mg of PCL-PEG-HA/FeCo/5-FU/CU, PCL-PEG-HA/FeCo/5-FU, and PCL-PEG-HA/FeCo/CU nanoparticles were added separately to 2 ml of PBS buffer and stored at 37 °C. The nanoparticles' supernatant was then collected by centrifugation (13,000 rpm for 1 hr) at predetermined time intervals and the nanoparticles were resuspended in 2 ml of PBS until the next collection. The amount of drug present in the supernatant was evaluated using spectrophotometry. The cumulative release percentage was then calculated using the following equation (Equation 1-2).

$$\text{Cumulative release percentage} = \frac{Dr^t + Dr^{t+1}}{DE}$$

Drt= The measured amount of drug in the supernatant at any time (t)
Drt+1= The measured amount of drug in the supernatant at time (t+1)
De= The amount of drug encapsulated in the nanoparticles

In vitro evaluation of cytotoxicity

The HCT116 colorectal cancer cell line was used to evaluate the toxicity and drug delivery efficiency of synthesized nanoparticles. First, Human Colorectal Carcinoma cell line HCT116 cells were grown in 10% fetal bovine serum and RPMI cell media at 37 °C in 5% CO_2. The Cytotoxic effect of Curcumin and 5-FU alone or together (5-FU and Curcumin) in colon cells was assessed by MTT reduction assay. For the MTT assay, 100 µl of HCT116 cells at a density of 7 ×104 cells per milliliter were transferred to 96-well plates. Then, the cells were kept in a CO_2 incubator (at 37 ° C, 90% humidity, and 5% CO_2) for 24 hr. The HCT116 cells were then treated with different concentrations of PCL-PEG-HA/FeCo/5-FU/CU nanoparticles (0, 25, 50, 75, 100, 200, and 400 µg/ml), as well as free 5-FU. To evaluate the toxicity of nanoparticles, PCL-PEG-HA/FeCo nanoparticles were used. To compare the efficiency of these nanoparticles in the drug delivery, the amount of Curcumin and 5-FU in each treatment was calculated in terms of the percentage of loading and final weight of the nanoparticles and in combination with each other on HCT116 cells. In order to calculate the toxicity of PCL-PEG-HA/FeCo, the amount of 5-FU and Curcumin were deducted from the number of treated nanoparticles, then a similar amount of PCL-PEG-HA/FeCo nanoparticles was added to each cell. The cells were exposed to each treatment for 24 hr. Then, the cell viability was assessed using MTT assay.

Cell Apoptosis Analysis Flow cytometer analysis with Annexin V-Dy634 KIT (Annexin V Apoptosis Detection Kit with PI, Immunostep company) was conducted to study the apoptosis response of HCT116 cells to Curcumin, 5-FU, and the combination. First, 6 cell plates were seeded by 3000 cells/ wall HCT116 cells and incubated for 24 hr at 37 °C, then cells were treated with the concentration of MTT test results (IC_{50} Values). After 48 hr incubation, the cells were rinsed with PBS buffer twice and then recollected from cells. The collected cells were centrifuged at 3000 rpm for 5 min and according to the manufacturer's instruction, the samples were treated with Annexin V and propidium iodide (PI) for 15 min at room temperature in a dark mood. The apoptosis detection kit Annexin V-FITC (BestBio; Nanjing Fengfeng Biological Medicine Technology Co., Ltd.) was utilized in accordance with the manufacturer's protocol for the assay. Subsequently, flow cytometry analysis (BD Accuri C6; BD Biosciences) was performed on the cells, and the data were processed using FlowJo™ software (version 10; FlowJo LLC).

RESULTS
Characterization of PCL-PEG-HA copolymer

The H-NMR spectra of PCL and PCL-PEG-HA copolymer are presented in Fig. 1. As shown in the H-NMR spectrum of PCL, Protons of -CH2- groups associated with PCL were present at 1.75 (b) and 3.42 (a) ppm. After the binding of PEG-HA to PCL, new peaks were observed in the range of 5.39 and 3.67 ppm, which were related to the PEG proton (c) and hyaluronic acid (d), respectively.
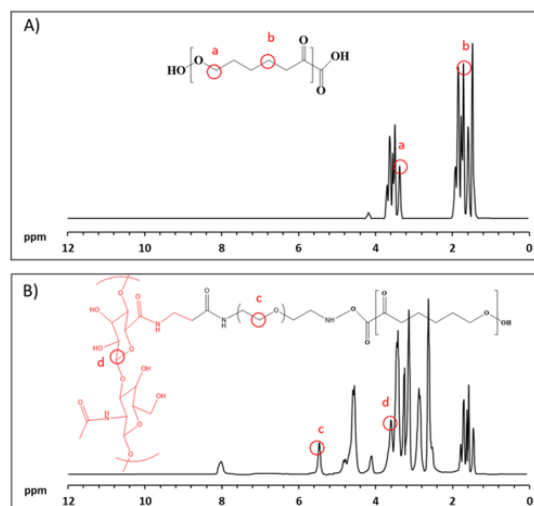

Fig. 1. The H-NMR spectra of A) PCL and B) PCL-PEG-HA and their schematic structure

The FT-IR spectra of PCL and PCL-PEG-HA copolymers shown in Fig. 2, confirmed the synthesis of PCL-PEG-HA. As shown in the FT-IR spectrum of PCL, the IR bands observed at 1846 cm^{-1} and 3104 cm^{-1} were related to C=O and C-H groups present in PCL. The FT-IR spectrum of PCL-PEG-HA copolymer revealed that strong peaks at 3286 cm^{-1} which was related to the hydroxyl group of PEG indicated the binding of the PEG-HA polymer to PCL. On the other hand, these results demonstrated a new band at 1612 cm^{-1} in PCL-PEG-HA copolymer, which was related to the N-H functional group of hyaluronic acid.

Thermogravimetric analysis (TGA) is an influential methodology employed to assess the thermal durability of various materials, encompassing polymers. Nonetheless, this
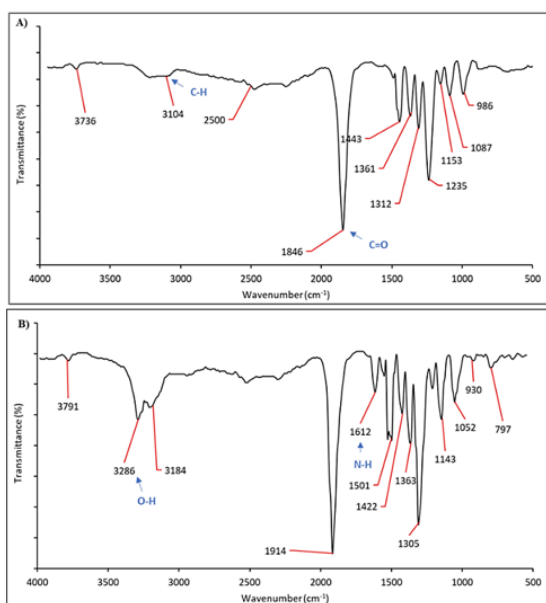
Fig. 2. The FT-IR spectra of A) PCL and B) PCL-PEG-HA.

observed in the TGA analysis of PLA-HA polymer in the temperature range of 200-250, 300-320, and 350-380 °C, which indicates the presence of several materials in PCL-PEG-HA compared to PCL. Considering that the weight loss of PCL was observed in the temperature range of 200 to 320 °C, it can be concluded that the weight loss in the temperature range of 350 to 380 °C is related to the hyaluronic acid present in the structure of PCL-PEG-HA copolymer.

Characterization of PCL-PEG-HA/FeCo/5-FU, PCL-PEG-HA/FeCo/CU and PCL-PEG-HA/FeCo/5-FU/CU nanoparticles

The results of studying the morphological properties and size of synthesized nanoparticles by transmission electron microscope (TEM) indicated that these nanoparticles had a spherical structure and a size of about 100-200 nm (Fig. 4). Furthermore, there are no significant differences between the shapes of nanoparticles. It has been determined that the efficiency of drug transfer to target tissues is related to the morphology of nanoparticles and that nanoparticles with a spherical structure have a high transfer efficiency among all types of spatial structures [36, 37].

The Dynamic light scattering (DLS) results

technique also possesses the capability to evaluate the proportion of components within a given sample. The TGA analysis of PCL, shown in Fig. 3, represents a severe weight loss stage which is indicative of the purity of the PCL polymer. On the other hand, several stages of weight loss were
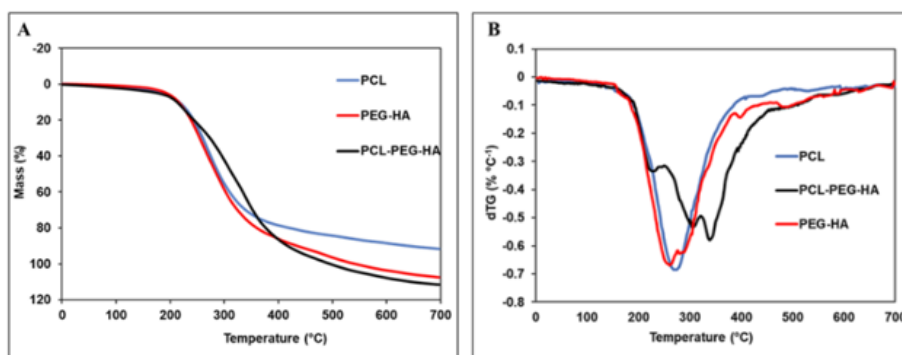

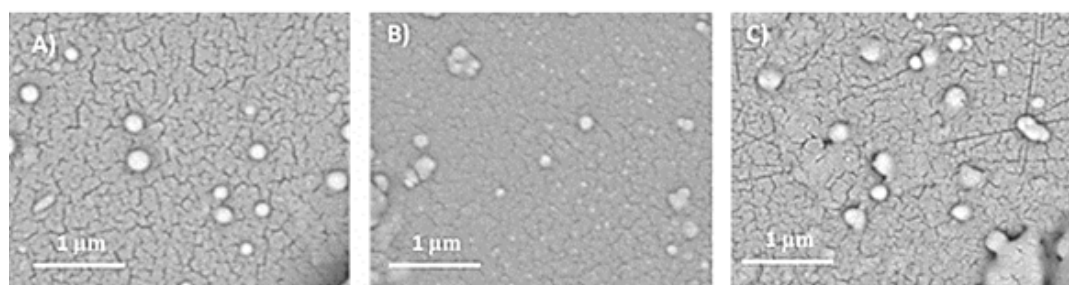Fig. 3. A) TGA and B) DTG analysis of A) PCL and B) PCL-PEG-HA.

Fig. 4. TEM image of PCL-PEG-HA/FeCO/5-FU, PCL-PEG-HA/FeCO/Curcumin and PCL-PEG-HA/FeCO/5-FU/Curcumin nanoparticles

shown in Fig. 5 confirmed the nanoscale dimensions of the synthesized nanoparticles. PCL-PEG-HA/FeCo/5-FU, PCL-PEG-HA/FeCo/CU and PCL-PEG-HA/FeCo/5-FU/CU nanoparticles were 193 ± 9.5, 218 ± 14.3, and 203 ± 6.9, respectively and there was no significant difference between the sizes of these nanoparticles.
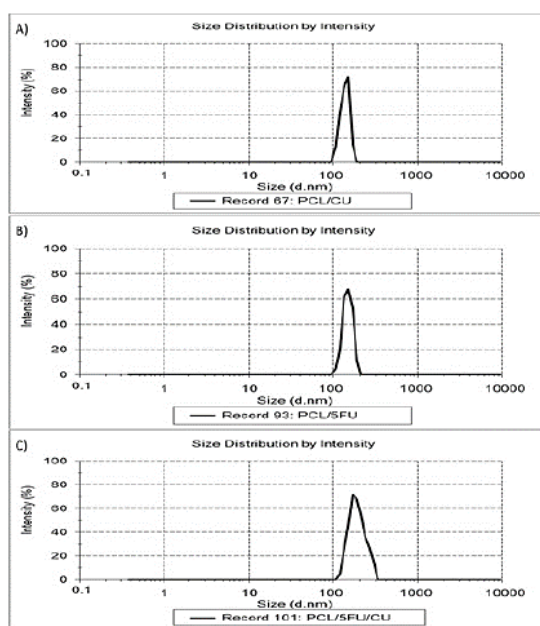

Fig. 5. The DLS results of synthesized nanoparticles

Fig. 6. The hysteresis curve of the synthesized nanoparticles

Graphical distribution of Zeta potential indicates the electrostatic stability of nanoparticles. Examining the results of the zeta potential of synthesized nanoparticles (PCL/CU, PCL/5-FU, and PCL/5-FU/CU) shows that the mentioned nanoparticles have an average negative charge (14.73±0.86, 20.08±0.35, and 11.12±0.44 mV, respectively) (Fig. 6).

The average size of nanoparticles (DLS) and the dispersion index PdI, which represents the size distribution and uniformity of the synthesized nanoparticles, are given in Table 1.

The hysteresis curve obtained from the vibrational sample magnetometer is demonstrated in Figure 7. The results confirmed that the magnetic property of PCL-PEG-HA/FeCo/FeCo nanoparticles was more than other nanoparticles and was 38 emu/g. With the encapsulation of 5-FU and Curcumin drugs, the magnetic saturation decreased in such a way that the lowest magnetic saturation in PCL-PEG-HA/FeCo/Curcumin/5-FU nanoparticles was observed and was 27 emu/g.
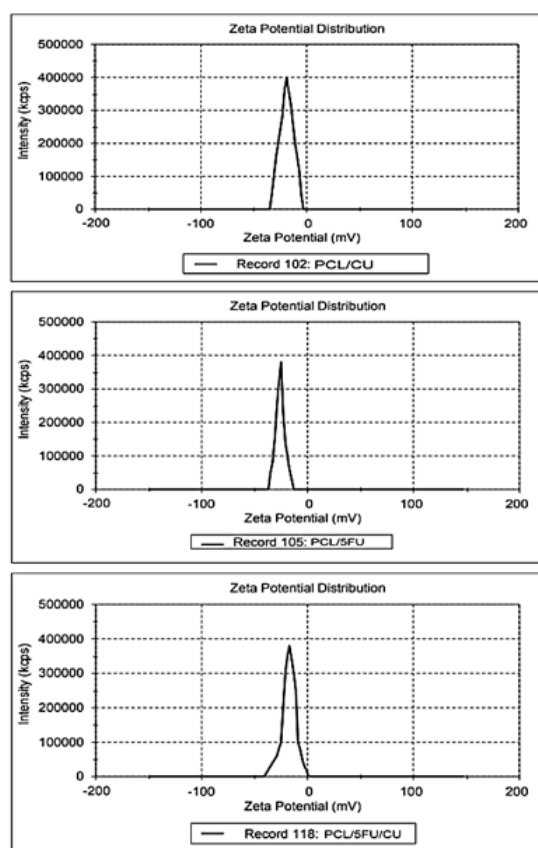
Table 1. Zeta potential, PDI, and particle size of PCL/5-FU, PCL/Curcumin, and PCL/5-FU/CU nanoparticles

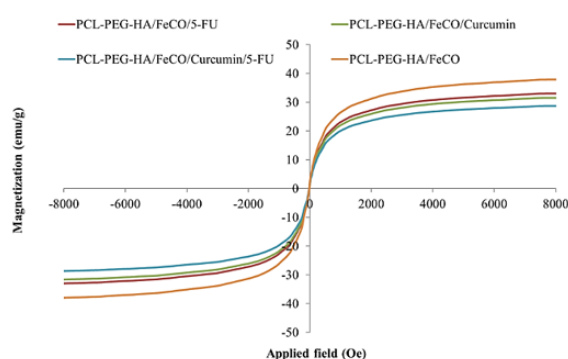| Nanoparticle	CU (%)	5-FU (%)
PCL-PEG-HA/FeCo/CU	35.9	-
PCL-PEG-HA/FeCo/5-FU	-	43.83
PCL-PEG-HA/FeCo/5-FU/CU	32.73	46.86

Fig. 7. Drug release profile of synthesized nanoparticles in acidic and neutral pH

Table 2. 5-FU and Curcumin Encapsulation efficiency in PCL-PEG-HA/FeCo copolymer

Nanoparticle	CU (%)	5-FU (%)
PCL-PEG-HA/FeCo/CU	35.9	-
PCL-PEG-HA/FeCo/5-FU	-	43.83
PCL-PEG-HA/FeCo/5-FU/CU	32.73	46.86

5-FU and Curcumin Encapsulation efficiency

According to the results, the encapsulation efficiency of Curcumin in PCL-PEG-HA/FeCo/Curcumin and PCL-PEG-HA/FeCo/5-FU/CU nanoparticles were 35.9 and 32.73, respectively. On the other hand, the encapsulation efficiency of 5-FU in PCL-PEG-HA/FeCo/5-FU and PCL-PEG-HA/FeCo/5-FU/CU nanoparticles were 43.83 and 46.86, respectively (Table 2). These results demonstrated that the 5-FU drug has a higher encapsulation efficiency than the Curcumin drug in PCL-PEG-HA/FeCo copolymer.

Drug release pattern

The results of evaluating the release pattern of PCL-PEG-HA/FeCo/5-FU/CU nanoparticles in neutral (pH=7.4) and acidic (pH=6) conditions showed that the release of 5-FU and Curcumin drugs takes place in two stages. In the first stage, the drug is released explosively. In fact, more than 50% of the total Curcumin drug released from PCL-PEG-HA/FeCo/CU nanoparticles was released only 3 days after incubation. However, more than 30% of the encapsulated 5-FU (PCL-PEG-HA/FeCo/5-

FU) was released only after 3 days of incubation, while the amount of drug released from PCL-PEG-HA/FeCo/5-FU/CU nanoparticles after 14 days of incubation in phosphate buffer and pH = 7.4, was 43.6% (Fig. 8).

The evaluation of the drug release of PCL-PEG-HA/FeCo/5-FU/CU nanoparticles in acidic conditions (pH=6) indicated that the release of both 5-FU and Curcumin drugs in acidic conditions was significantly higher than the drug release in the neutral pH (7.4). For example, the amount of Curcumin drug released from PCL-PEG-HA/FeCo/5-FU/CU nanoparticles in 14 days at pH=7.4 was 57.36%, while this amount increased to more than 75% at pH=6.

In vitro cytotoxicity

In this study, in order to increase the efficiency of targeted drug delivery to colorectal HCT116 cancer cells, the PCL polymer surface was coated with PEG-HA. In addition, the ability to transport Curcumin and 5-FU drugs through these nanoparticles and their effect (Together and separately) on the viability of HCT116 cells was also evaluated through the MTT test.

According to findings, the highest IC50 value of HCT116 cells (122.2 mg/L) was associated with PCL-PEG-HA/FeCo treatment. The lowest value of Half-maximal inhibitory concentration (IC_{50}) (64.42 mg/L) is related to the combined treatment of curcumin and 5-Fu. Based on the results obtained, the synthesized nanoparticles had the least impact
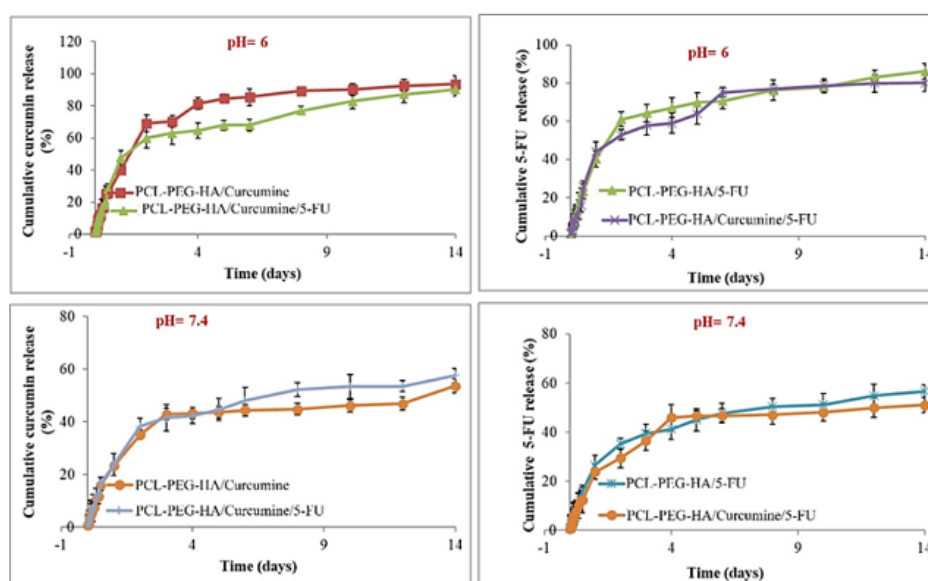

Fig. 8. Drug release profile of synthesized nanoparticles in acidic and neutral pH
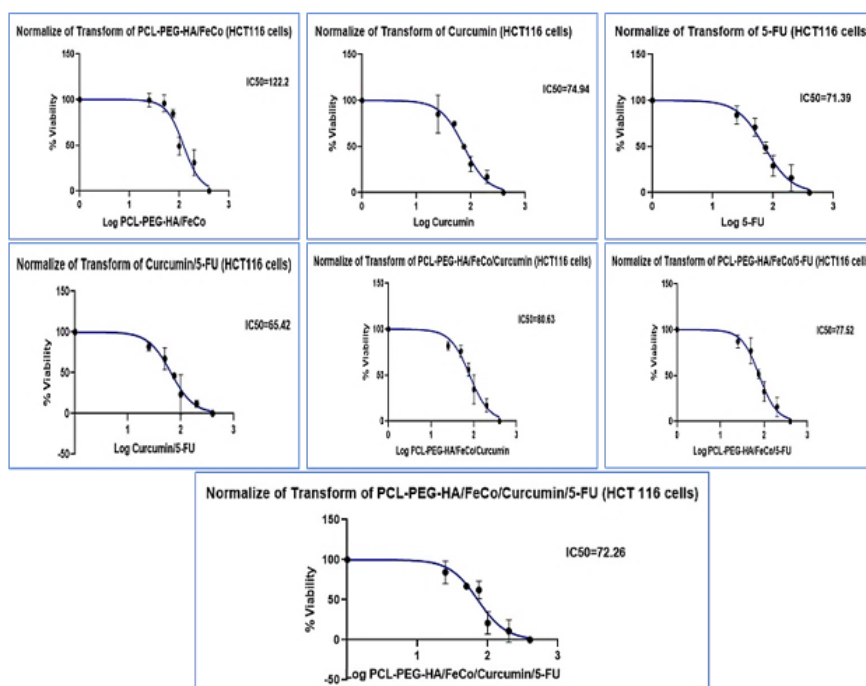
Fig. 9. IC$_{50}$ value of HCT116 colorectal cells

on cell viability. Furthermore, according to the results obtained (Fig. 10), there was a difference between the IC$_{50}$ value of the drug and the drug-coated nanoparticle, so using the drug without nanoparticles reduces the IC$_{50}$ value of the target cells (Table 3). It can be concluded that coating the drug with nanoparticles results in slow release of the drug in the culture medium and long-term effect of the drug (Fig. 9).

Cell apoptosis analysis

The biological process of regulating cell numbers is called apoptosis, which is a naturally occurring type of programmed cell death. Cell shrinkage, chromatin condensation, membrane blebbing, and the emergence of distinctive nuclear bodies are their morphological hallmarks (38). Despite the fact that apoptosis happens naturally, it can also be brought on by a variety of bodily processes and outside stimuli, including ionizing

radiation (39). This investigation into the apoptosis of cancer cells used the flow cytometry test with annexin V and PI. The findings of this investigation demonstrated that the presence of PCL-PEG-HA/FeCo/5-FU/CU nanoparticles significantly increased both early and late apoptosis in the colorectal cancer cell line HCT 116 (4.33 and 17.17 percent, respectively). which, was significantly higher (at 1% probability level) compared to other treatments. As can be seen in Fig. 10, there is no statistically significant difference between the drug-free nanoparticle as a control treatment (PCL-PEG-HA/FeCo) and free curcumin /free 5-FU (without nanoparticles) in terms of the percentage

Table 3. Analysis of variance of Ic$_{50}$ (Dunkan) value

S.O.V	MS	
	df	Ic$_{50}$
Treatment	6	1016.86 **
Error	14	4.84
CV(%)	-	2.77

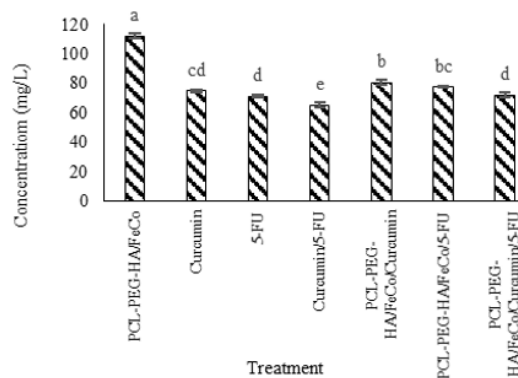**: significant at 1% probability level

Fig. 10. Comparison of the value of IC$_{50}$ (mg/L) of HCT 116 colorectal cancer cells based on different treatments
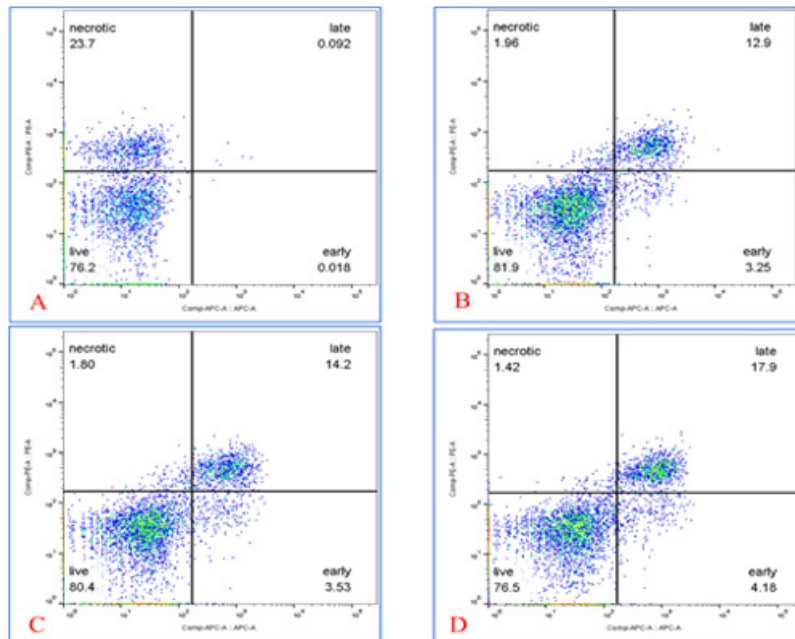
Fig. 11. Cell apoptosis of treated HCT 116 Colorectal cancer; A: Control, B: Nanoparticle (PCL-PEG-HA/FeCo), C: Drugs (5-FU+ CUR), D: Nanoparticles + drugs (PCL-PEG-HA/FeCo/5-FU/CU)

of early apoptosis and late apoptosis (Fig. 11). On the other hand, coated drugs in nanoparticles (separately) and the combination of drugs (PCL-PEG-HA/FeCo/5-FU/CU, PCL-PEG-HA/FeCo/CU, and PCL-PEG-HA/FeCo/5- FU) had caused a significant increase in the probability level of 1% in early apoptosis and late apoptosis of HCT 116 cell lines of colorectal cancer.

In terms of the necrotic rate of HCT 116 cell line samples, a statistically significant difference was observed between the treatments. The drug-free treatment (control nanoparticle) had the highest amount of cell necrosis (24.17%), which can be the result of the unrestricted growth of cells in the cell culture medium and high level of death due to cell density (40) which in other experimental treatments, due to increase in apoptosis rate, there was a decrease in cell density and result the percentage of cell necrosis has decreased significantly compared to the control treatment (Fig. 12).
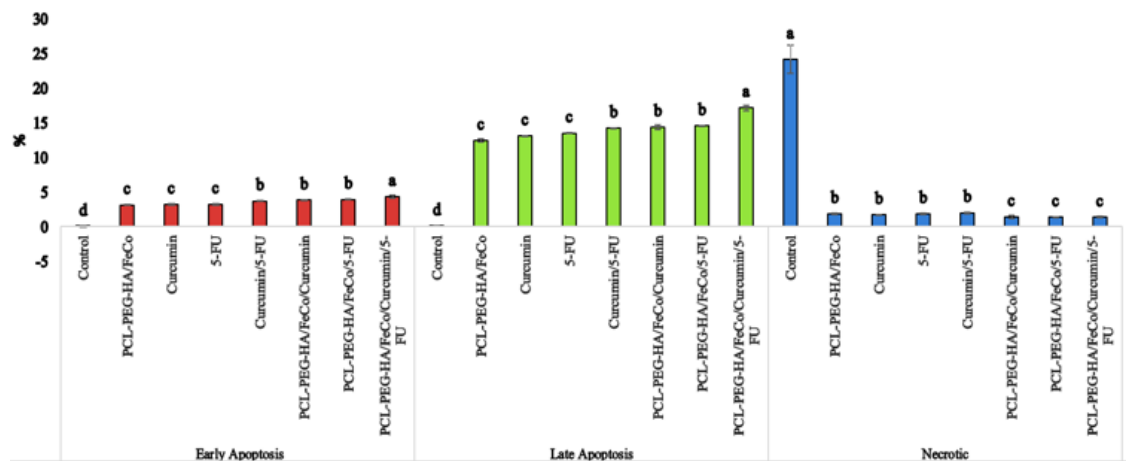

Fig. 12. Comparison of apoptosis analysis; Necrotic, Early apoptosis, and Late apoptosis percentages in different treatments on HCT 116 Colorectal cancer cells

DISCUSSION

Particle size and the surface charge are responsible for a wide range of biological functions in nanoparticles, including bio distribution, toxicity (41) cellular uptake (42), and dissolution (43). Therefore, it is necessary to investigate these two factors during the development of nanoparticles in drug delivery systems. Previous studies have shown that, nanoparticles with particle size in the range of 100–200 nm tend to accumulate in tumor tissues much more, in comparison to normal cells (44). Some studies have demonstrated that nanoparticles with diameters less than 200 nm have a higher ability, to escape uptake using the reticuloendothelial system (RES) compared to nanoparticles with larger particle sizes (45). In line with the findings of prior investigations, reducing the size of nanoparticles increases the probability of successful delivery to cancer cells, while indiscriminate uptake by healthy cells is enhanced for nanoparticles below 50 nm in size. To further explain, reducing the size of nanoparticles to less than 50 nm not only increases the transduction efficiency but also increases the incidence of side effects in the form of non-specific uptake by healthy cells(46). Based on the findings, nanoparticles measuring 200 nm in size are deemed to be a viable alternative for the targeted delivery of drugs to cancerous tissues. This particular group of nanoparticles exhibis enhanced transfer efficiency owing to their size being less than 200 nm, and the nonspecific uptake of these nanoparticles by normal cells is comparatively lower than that of nanoparticles measuring less than 100 nm in size. In light of the results obtained from this investigation, it can be inferred that the size of the PCL-PEG-HA/FeCo/CU/5-FU nanoparticles ranged around 200 nm, thereby implying that these nanoparticles possess the superior capability to penetrate cancer cells while simultaneously exhibiting minimal uptake by normal cells in vivo. In a study conducted by Noor Alam and colleagues, aimed at the development and characterization of cisplatin-loaded PLGA-HA nanoparticles, a slight increase in the size of hyaluronic acid-conjugated nanoparticles was observed in comparison to PLGA nanoparticles. The plausible explanation for this size increment lies in the presence of hyaluronic acid segments. Furthermore, this study revealed that the HA-containing nanoparticles displayed a more negative zeta potential, which can be attributed to the presence of negative carboxyl groups within the hyaluronic acid molecule (47). In a similar vein, Serri et al. conducted a study on the preparedness of PLGA nanoparticles that incorporated hyaluronic acid on their exterior. The researchers observed a 30% increase in size when comparing these nanoparticles to those without hyaluronic acid. Furthermore, Serri et al. posited that the diffusion of drugs into the nanoparticles contributes to their size augmentation, as it leads to the expansion of the inner liquid phase. Additionally, this review regarded the manifestation of deficient zeta potential in hyaluronic acid-containing nanoparticles as evidence of the presence of hyaluronic acid on the nanoparticle surface(48).

It has been reported that zeta potential is a very important key to determine the cellular uptake efficiency and the in-vivo fate of nanoparticles (49). However, the optimum surface charges (e.g. negative, neutral or positive) and surface charge densities were reported differently for different types of drug delivery systems, in order to prolong the plasma circulation time of nanoparticles, minimize the nonspecific binding of nanoparticles and prevent their loss to nontarget locations. For example, Yamamoto et al. (50) demonstrated that negatively charged PEG-PDLLA nanoparticles exhibited no significant difference in nanoparticles blood clearance kinetics; however, the negative surface charge of nanoparticles remarkably reduced the nonspecific uptake by spleen and liver, which was due to the electrostatic repulsion between negatively charged plasma membrane of the cells and nanoparticles. Conversely, Juliano et al. reported that the positively charged nanoparticles were cleared less rapidly compared to negatively charged ones, which was attributed to the tendency of negatively charged nanoparticles to coalesce in the presence of calcium ions and proteins in blood plasma (51).

The tumor microenvironment is characterized by low pH, low oxygen, and high redox. The pH in the extracellular tissues and blood remained around 7.4. Due to the high glycolysis rate of tumor cells, the pH decreased to 6.2–6.8 and even decreased to 4.5–5.5 in the endosomes/lysosomes (52). Based on the pH gradient, acid-triggered drug release nano drug-sustained systems would be arranged to show a responsive release mechanism to the tumor microenvironment. In the neutral environment, nanoparticles generally exist in uniform morphology and almost do not

show drug-release behavior (53). However, in acidic conditions, the drug release phenomenon may occur abruptly, which improves the targeted drug release. pH-responsive release often results from the breaking of specific chemical bonds. For example, imine bonds are stable under neutral conditions but break under acidic conditions, and targeted release can be achieved when the connection between drug and carrier is broken (54). In addition, charge interaction, hydrophobic interaction, and morphology of the particles also have a great influence on drug release. Some natural and synthetic copolymers are sensitive to pH such as HA and PEG. These copolymers respond to the changes in the pH of the surrounding medium by varying their dimensions. These copolymers may swell, collapse, or disintegrate depending on the pH of the environment (55). This behavior is exhibited due to the presence of certain functional groups in the polymer chain. pH-sensitive materials can be either acidic or basic, responding to either basic or acidic pH values. The aim of assessing the release characteristics of the nanocarrier was to guarantee its sensitivity to changes in pH and its capacity to provide a continuous release of medication. One key aspect in the liberation of drugs encapsulated within nanoparticles is to replicate optimal and comparable conditions to those found within the human body in a controlled laboratory setting, as the ultimate destination for transfer is the patient's body. Phosphate buffer solution (PBS) with a pH value of 7.4 is a relatively stable compound that closely resembles the acidity levels found within the human body, and as such, it is commonly employed in various biological experiments. Studies have indicated that cancer cells possess a slightly higher degree of acidity compared to normal body tissue (pH=6) (56). Therefore, in the current investigation, to direct drug transportation to cancerous cells and investigate the pattern of drug liberation, phosphate buffer was used. Empirical research has demonstrated that the liberation of drugs from micellar nanoparticles emerges from an analogous pattern, and the scientific community concurs that the rationale behind this phenomenon is the encapsulation of the drug within the outer layers of this particular assemblage of nanoparticles. This encapsulation is primarily instigated by the augmented contact area between the drug and the phosphate buffer, leading to an abrupt escalation in the magnitude

of drug liberation. Nonetheless, the release of drugs located within the central regions of nanoparticles requires a lengthier period of time (57). The investigation of the drug release pattern from the synthesized nanoparticles in acidic conditions (pH=6) revealed that the release of 5-FU and Curcumin was greater in comparison with the release in neutral conditions. The accelerated degradation of the nanoparticles in acidic conditions leads to a faster release of the drugs. Previous studies have also explored the release of drugs from polymer nanoparticles with a magnetic core. A study conducted by Amani et al. examined the design and evaluation of iron oxide nanoparticles coated with a PLA-PEG-PLA copolymer and observed both burst and continuous release patterns of drug release in neutral and acidic environments. Under similar conditions, the rate of drug release from nanoparticles was significantly higher in an acidic medium as compared to a neutral medium. This study delved into the chemical and biochemical processes involved in the separation of drugs from nanoparticles, as well as the rationale behind the disparity in release rate between an acidic and a neutral environment. Furthermore, it was noted that the process of drug release from nanoparticles generally proceeds at a slower pace in a neutral climate as opposed to an acidic climate. Given that cancer cells or tumor tissues exhibit a lower pH compared to healthy cells or tissues, a higher release rate into acidic tissues may result in reduced side effects compared to the use of free drugs (58). In recent times, the joint administration of naturally occurring substances, which have been confirmed to possess anti-cancer properties, through the implementation of combinatorial chemotherapy, has been the subject of investigation within clinical environments. The impact of Cur, in terms of its ability to diminish telomerase activity, has been observed in numerous cancerous cell lines, as indicated by an escalating quantity of scientific publications (59). This reduction was found to be due to the blocking of the nuclear localization of telomerase by the separation of the chaperone Hsp90p23 complex from Telomerase Reverse Transcriptase (TERT) and thus to the inhibition of the translocation of TERT to the nucleus. The interaction of Hsp90 and p23 with hTERT is essential for the regulation of nuclear transport of telomerase (60). Furthermore, downregulation of TERT expression by Cur results

in the suppression of telomerase activity, with increasing concentrations of Cur leading to decreased TERTmRNA levels while TR mRNA levels remain unchanged (61). 5-FU is a widely used drug in the first-line treatment of colorectal cancer (62). Over 80% of the administered 5-FU dose is rapidly metabolized and only 13% is converted to its active metabolite FdUMP. FdUMP then inhibits thymidylate synthase (TYMS, OMIM: 188350) and blocks deoxythymidine triphosphate (dTTP) synthesis. Subsequent dTTP depletion triggers death without thymine (63). TYMS is considered a potential prognostic marker for colorectal cancer. Recent studies have shown that overexpression of the TYMS transcript predicts poor outcomes in patients with colorectal cancer (64). Several investigations have put forward the notion that the expression of enzymes involved in the metabolism of 5-FU may have a potential prognostic or predictive function in the resistance to treatment observed in colorectal cancer. Patients afflicted with colorectal cancer who exhibit diminished protein expression of the 5-FU-inactivating enzyme, namely dihydropyrimidine dehydrogenase (DPYD, OMIM: 612778), have been found to experience longer survival periods following 5-FU treatment in comparison to those patients who possess elevated levels of this enzyme (65, 66). Likewise, high DPYD transcript level was associated with poor outcome in stage IV colorectal cancer patients (67). High transcript level of TYMP was associated with significantly better disease-free survival (DFS) after oral administration of 5-FU in patients with stage III colorectal cancer (68, 69). The action of CUR was determined to have a synergistic effect in the improvement of 5-FU efficacy through the inhibition of cytochrome c oxidase subunit II (COX2) overexpression in colorectal cancer. Within the scope of this study, it was demonstrated that the combined treatment of CUR and 5-FU loaded in PCL-PEG-HA nanoparticles resulted in an augmentation of the anticancer effects against HCT116 cells when compared to the effects of individual treatments. Furthermore, it was observed that a low concentration of curcumin had the ability to enhance the anticancer effect of 5-fluorouracil against HCT116 cells in colorectal cancer (70). Due to the inherent hydrophilicity of polyethylene glycol PEG and the hydrophobicity of polycaprolactone PCL, PCL-PEG-HA/FeCo copolymers have been utilized to enhance the efficiency of drug delivery to HCT116 cells. This is further facilitated by the interaction between hyaluronic acid within the nanoparticle structure and cell surface adhesion receptor (CD44) receptors, which are known to be overexpressed on the surface of the HCT116 cell membrane. In a study conducted by Ni et al., the efficacy of docetaxel in combating colorectal cancer was improved through the use of dual-modified PCL-PEG nanoparticles. The findings of this study indicate that the incorporation of docetaxel into PCL-PEG-based nanoparticles enables precise targeting of colorectal cancer cells and efficient drug delivery, thus leading to enhanced antitumor activity. It is plausible to consider that this nanomedicine platform can be readily extended to other cancer types by modifying the chemotherapeutic agents and the targeted components. Therefore, this dual targeting nanomedicine platform exhibits promising potential for the delivery of anticancer drugs in future nanomedicine applications (71). Furthermore, within a novel investigation, a polymeric drug delivery system consisting of HA-functionalized camptothecin (CPT)/ CUR-loaded polymeric NPs (HA-CPT/CUR-NPs) was utilized for the purpose of delivering curcumin to cancerous cells. Through cellular uptake experiments, it was observed that the incorporation of HA into the NP surface conferred upon the NPs the capability to combat colon cancer and notably enhance the efficiency of cellular uptake in comparison to NPs coated with chitosan. Significantly, the concurrent delivery of CPT and CUR within a HA-functionalized NP exhibited potent synergistic effects. It was ascertained that the introduction of HA as a targeting component in nanoparticles could elevate their cytotoxicity by virtue of the specific interactions occurring between hyaluronic acid and the over-expressed CD44 receptor on the surface of colorectal cancer cells (72). Both 5-Fu and Curcumin are valuable chemotherapy agents, and while they have limited bioavailability, to overcome these limits, in some studies, researchers have co-delivered them. Sadeghi-Abandansari et al., (2021) conducted an experiment to investigate 5-FU in combination with curcumin for colon cancer. According to their results, combined drug formulation enhanced their anticancer effects against colon cancer cells (HT-29). Also they proved the synergistic inhibitory of 5-Fu and Curcumin effects on the cell cycle progression and cell

proliferation in HT-29 cells (73).

One of the most important processes that cells use to maintain their life activities is called cell apoptosis, or programmed cell death (74). Proteins known as caspases, or cysteine aspartate-specific proteinases, are essential for promoting programmed cell death. These proteins play a crucial role in initiating the process of cell destruction (75). Cancer cells can undergo apoptosis through the action of three different signaling pathways: the death receptor, mitochondrial, and endoplasmic reticulum pathways (76). The most significant of these pathways is the Fas receptor-mediated apoptosis pathway. The cancer stem cell theory of tumor growth suggests that Fas signaling is involved in senescence, tumor maintenance, and cell apoptosis. Several studies have indicated that curcumin has the ability to suppress the proliferation of cancer cells and induce apoptosis in these cells employing cell cycle arrest mediated by p21. Conversely, it is believed that the signaling cascades of Mitogen-activated protein kinase (MAPK) and NF-kappa B (NFκB) play a role in regulating apoptosis and cell survival. Although curcumin inhibits NFκB, its impact on the MAPK pathways remains uncertain (77). Furthermore, the activation of caspase-6 by 5-FU may trigger apoptosis in cancer cells. Additionally, in the p53-dependent pathway, 5-FU generates mitochondrial ROS (78). These findings are in line with the results of our experiment that increase the amount of cell apoptosis (early and late). Therefore, the synergistic effect of curcumin and 5-Fu drugs with targeted transfer by nanoparticles can increase cell apoptosis, targeted and controlled transfer (change of drug release pattern) and can be considered as one of the effective and efficient ways in the treatment of colorectal cancer. By modifying the released cytokines and chemokines, polarizing pro-tumor and anti-tumor cells, and ultimately causing anti-tumor cells to release dead signals, curcumin can control immune responses (79). Apoptosis in cancer cells is induced by an increase in the activity of NK cells and CTLs, whereas antitumor cell apoptosis and cancer cell resistance to apoptosis are linked to the infiltration of Tregs, TAMs, and CAFs (80). Curcumin has been demonstrated to lessen NK cell apoptosis. NK cells undergo apoptosis stimulation and NF-κB downregulation as a result of their interactions with immunosuppressive cells within tumors. Increased Treg activation is linked to this.

NK cells' decreased NF-κB level can be reversed by curcumin, preventing NK cells from dying. It has also been demonstrated that curcumin increases the cytotoxicity of natural killer (NK) cells against cancerous cells by inducing a greater release of interferon-γ (IFN-γ) (81).

As a consequence, PCL-PEG-HA/FeCo/5-FU/Curcumin nanoparticles can be an efficient solution in targeted drug delivery due to their physicochemical properties and release profile, toxicity, and proper efficiency in transferring 5-FU and curcumin to colorectal cancer cells.

CONCLUSION

As described above, 5-Fu and Curcumin are of main drugs for chemotherapy of colorectal cancer, due to their limited biocompatibility, targeted drug delivery by nanoparticles such as PCL-PEG-HA/FeCo are used to overcome their limits. These methods lead to increase the effect of chemotherapy drugs and their targeted transfer to cancer cells. On the other hand, by changing the drug release pattern and targeted delivery, the side effects of drugs and their effects on healthy cells are reduced. Nanoparticles and their use in targeted drug delivery systems are one of the promising methods to treat cancer.

CONFLICTS OF INTEREST

The authors declare that there is no conflict of interest.

REFRENCES

1. Sawicki T, Ruszkowska M, Danielewicz A, Niedźwiedzka E, Arłukowicz T, Przybyłowicz KE. A review of colorectal cancer in terms of epidemiology, risk factors, development, symptoms and diagnosis. Cancers. 2021;13(9):2025.
2. Levy MH, Back A, Benedetti C, Billings JA, Block S, Boston B, et al. NCCN clinical practice guidelines in oncology: palliative care. J Natl Compr Canc Netw. 2009;7(4):436-473.
3. Van Cutsem E, Cervantes A, Adam R, Sobrero A, Van Krieken J, Aderka D, et al. ESMO consensus guidelines for the management of patients with metastatic colorectal cancer. Ann Oncol. 2016;27(8):1386-1422.

4. Chibaudel B, Tournigand C, Bonnetain F, Richa H, Benetkiewicz M, André T, de Gramont A. Therapeutic strategy in unresectable metastatic colorectal cancer: an updated review. Ther Adv Med Oncol. 2015;7(3):153-169.

5. Wen Y, Chen X, Zhu X, Gong Y, Yuan G, Qin X, Liu J. Photothermal-chemotherapy integrated nanoparticles with tumor microenvironment response enhanced the induction of immunogenic cell death for colorectal cancer efficient treatment. ACS Appl Mater Interfaces. 2019;11(46):43393-408.

6. Kalyan A, Kircher S, Shah H, Mulcahy M, Benson A. Updates on immunotherapy for colorectal cancer. J Gastrointest Oncol. 2018;9(1):160.

7. Papadimitriou M, Papadimitriou CA. Antiangiogenic tyrosine kinase inhibitors in metastatic colorectal cancer: focusing on regorafenib. Anticancer Res. 2021;41(2):567-582.

8. Dasineh S, Akbarian M, Ebrahimi HA, Behbudi G. Tacrolimus-loaded chitosan-coated nanostructured lipid carriers: preparation, optimization and physicochemical characterization. Appl Nanosci. 2021;11:1169-1181.

9. Vodenkova S, Buchler T, Cervena K, Veskrnova V, Vodicka P, Vymetalkova V. 5-fluorouracil and other fluoropyrimidines in colorectal cancer: Past, present and future. Arch Pharmacol Ther. 2020;206:107447.

10. Cho Y-H, Ro EJ, Yoon J-S, Mizutani T, Kang D-W, Park J-C, et al. 5-FU promotes stemness of colorectal cancer via p53-mediated WNT/β-catenin pathway activation. Nat Commun. 2020;11(1):5321.

11. Christensen S, Van der Roest B, Besselink N, Janssen R, Boymans S, Martens JW, et al. 5-Fluorouracil treatment induces characteristic T> G mutations in human cancer. Nat Commun. 2019;10(1):4571.

12. Chionh F, Lau D, Yeung Y, Price T, Tebbutt N. Oral versus intravenous fluoropyrimidines for colorectal cancer. Cochrane Database Syst Rev. 2017; 2017(7): CD008398.

13. Lin SR, Chang CH, Hsu CF, Tsai MJ, Cheng H, Leong MK, et al. Natural compounds as potential adjuvants to cancer therapy: Preclinical evidence. Br J Pharmacol. 2020;177(6):1409-1423.

14. Xu Z, Hu C, Chen S, Zhang C, Yu J, Wang X, et al. Apatinib enhances chemosensitivity of gastric cancer to paclitaxel and 5-fluorouracil. Cancer Manag Res. 2019:4905-4915.

15. Wang J, Qiao Y, Sun M, Sun H, Xie F, Chang H, et al. FTO promotes colorectal cancer progression and chemotherapy resistance via demethylating G6PD/PARP1. J Clin Transl Sci. 2022;12(3): e772.

16. Karthika C, Hari B, Rahman MH, Akter R, Najda A, Albadrani GM, et al. Multiple strategies with the synergistic approach for addressing colorectal cancer. Biomed Pharmacother. 2021;140:111704.

17. Song L, Hao Y, Wang C, Han Y, Zhu Y, Feng L, et al. Liposomal oxaliplatin prodrugs loaded with metformin potentiate immunotherapy for colorectal cancer. J Control Release. 2022;350:922-932.

18. Xiao Q, Xiao J, Liu J, Liu J, Shu G, Yin G. Metformin suppresses the growth of colorectal cancer by targeting INHBA to inhibit TGF-β/PI3K/AKT signaling transduction. Cell Death Dis. 2022;13(3):202.

19. Davis SL, Hartman SJ, Bagby SM, Schlaepfer M, Yacob BW, Tse T, et al. ATM kinase inhibitor AZD0156 in combination with irinotecan and 5-fluorouracil in preclinical models of colorectal cancer. BMC cancer. 2022;22(1):1107.

20. Patil SS, Bhasarkar S, Rathod VK. Extraction of curcuminoids from Curcuma longa: comparative study between batch extraction and novel three phase partitioning. Prep Biochem Biotechnol. 2019;49(4):407-418.

21. Sharifi-Rad J, Rayess YE, Rizk AA, Sadaka C, Zgheib R, Zam W, et al. Turmeric and its major compound curcumin on health: bioactive effects and safety profiles for food, pharmaceutical, biotechnological and medicinal applications. Front Pharmacol. 2020;11:1021.

22. Talib WH, Alsalahat I, Daoud S, Abutayeh RF, Mahmod AI. Plant-derived natural products in cancer research: extraction, mechanism of action, and drug formulation. Molecules. 2020;25(22):5319.

23. Su P, Yang Y, Wang G, Chen X, Ju Y. Curcumin attenuates resistance to irinotecan via induction of apoptosis of cancer stem cells in chemoresistant colon cancer cells. Int J Oncol Res. 2018;53(3):1343-1353.

24. Ojo OA, Adeyemo TR, Rotimi D, Batiha GE-S, Mostafa-Hedeab G, Iyobhebhe ME, et al. Anticancer properties of curcumin against colorectal cancer: a review. Front Oncol. 2022;12:881641.

25. Weng W, Goel A, editors. Curcumin and colorectal cancer: An update and current perspective on this natural medicine. Semin Cancer Biol; 2022: Elsevier.

26. Marjaneh RM, Rahmani F, Hassanian SM, Rezaei N, Hashemzehi M, Bahrami A, et al. Phytosomal curcumin inhibits tumor growth in colitis-associated colorectal cancer. J Cell Physiol. 2018;233(10):6785-6798.

27. Yaghoubi H, Eskanlou H, Danandeh Baghrabad M, Farazi N, Nedaee Shakarab B. Preparation and evaluation of anti-cancer effects of targeted polymer nano particles containing paclitaxel and siRNA in MCF-7 breast cancer cell line. Cell Mol Biol. 2023.

28. Sukumaran S, Neelakandan M, Shaji N, Prasad P, Yadunath V. Magnetic nanoparticles: Synthesis and potential biological applications. JSM Nanotechnology & Nanomedicine. 2018;6(2):1068.

29. Abdolmaleki A, Khudhur ZO, Smail SW, Asadi A, Amani A. FeCo-Chitosan/DNA nanoparticles for gene transfer to MCF-7 breast cancer cells: preparation and characterization. Breast Cancer (Auckl). 2021;13(4):245-257.

30. Sami El-banna F, Mahfouz ME, Leporatti S, El-Kemary M, AN Hanafy N. Chitosan as a natural copolymer with unique properties for the development of hydrogels. World Appl Sci J. 2019;9(11):2193.

31. Archer E, Torretti M, Madbouly S. Biodegradable polycaprolactone (PCL) based polymer and composites. Phys Sci Rev. 2021(0):000010151520200074.

32. Afrouz M, Ahmadi-Nouraldinvand F, Ajirlu YY, Arabnejad F, Eskanlou H, Yaghoubi H. Preparation and characterization of PLA-PEG/Chitosan-FA/DNA for gene transfer to MCF-7 cells. Med Drug Discov. 2022;15:100138.

33. Guastaferro M, Baldino L, Cardea S, Reverchon E. Supercritical processing of PCL and PCL-PEG blends to produce improved PCL-based porous scaffolds. J Supercrit Fluids. 2022;186:105611.

34. Afrouz M, Ahmadi-Nouraldinvand F, Amani A, Zahedian H, Elias SG, Arabnejad F, et al. Preparation and characterization of magnetic PEG-PEI-PLA-PEI-PEG/Fe$_3$O$_4$-PCL/DNA micelles for gene delivery into MCF-7 cells. J Drug Deliv Sci Technol. 2023;79:104016.

35. Fu C-P, Cai X-Y, Chen S-L, Yu H-W, Fang Y, Feng X-C, et al. Hyaluronic Acid-Based Nanocarriers for Anticancer Drug Delivery. Polymers. 2023;15(10):2317.

36. Trang NTT, Chinh NT, Giang NV, Thanh DTM, Lam TD, Thu LV, et al. Hydrolysis of green nanocomposites of poly (lactic acid)(PLA), chitosan (CS) and polyethylene glycol

(PEG) in acid solution. Green Processing and Synthesis. 2016;5(5):443-449.

37. Prabha G, Raj V. Preparation and characterization of chitosan—Polyethylene glycol-polyvinylpyrrolidone-coated superparamagnetic iron oxide nanoparticles as carrier system: Drug loading and in vitro drug release study. J Biomed Mater Res B Appl Biomater. 2016;104(4):808-816.

38. Pietkiewicz S, Schmidt JH, Lavrik IN. Quantification of apoptosis and necroptosis at the single cell level by a combination of Imaging Flow Cytometry with classical Annexin V/propidium iodide staining. J Immunol Methods. 2015;423:99-103.

39. Pérez-Garijo A, Fuchs Y, Steller H. Apoptotic cells can induce non-autonomous apoptosis through the TNF pathway. Elife. 2013;2:e01004.

40. Gao W, Wang X, Zhou Y, Wang X, Yu Y. Autophagy, ferroptosis, pyroptosis, and necroptosis in tumor immunotherapy. Signal Transduct Target Ther. 2022;7(1):196.

41. Khan I, Saeed K, Khan I. Nanoparticles: Properties, applications and toxicities. Arab J Chem. 2019;12(7):908-931.

42. Nam S-H, An Y-J. Size-and shape-dependent toxicity of silver nanomaterials in green alga Chlorococcum infusionum. Ecotoxicol Environ Saf. 2019;168:388-393.

43. Mendes RG, Koch B, Bachmatiuk A, El-Gendy AA, Krupskaya Y, Springer A, et al. Synthesis and toxicity characterization of carbon coated iron oxide nanoparticles with highly defined size distributions. Biochim Biophys Acta Gen Subj. 2014;1840(1):160-169.

44. Mosquera J, García I, Liz-Marzán LM. Cellular uptake of nanoparticles versus small molecules: a matter of size. Acc Chem Res. 2018;51(9):2305-2313.

45. Bai X, Wang S, Yan X, Zhou H, Zhan J, Liu S, et al. Regulation of cell uptake and cytotoxicity by nanoparticle core under the controlled shape, size, and surface chemistries. ACS nano. 2019;14(1):289-302.

46. Shieh M-J, Peng C-L, Lou P-J, Chiu C-H, Tsai T-Y, Hsu C-Y, et al. Non-toxic phototriggered gene transfection by PAMAM-porphyrin conjugates. J Control Release. 2008;129(3):200-206.

47. Alam N, Koul M, Mintoo MJ, Khare V, Gupta R, Rawat N, et al. Development and characterization of hyaluronic acid modified PLGA based nanoparticles for improved efficacy of cisplatin in solid tumor. Biomed Pharmacother. 2017;95:856-864.

48. Serri C, Quagliariello V, Iaffaioli RV, Fusco S, Botti G, Mayol L, Biondi M. Combination therapy for the treatment of pancreatic cancer through hyaluronic acid-decorated nanoparticles loaded with quercetin and gemcitabine: A preliminary in vitro study. J Cell Physiol. 2019;234(4):4959-4969.

49. He C, Hu Y, Yin L, Tang C, Yin C. Effects of particle size and surface charge on cellular uptake and biodistribution of polymeric nanoparticles. Biomaterials. 2010;31(13):3657-3666.

50. Yamamoto Y, Nagasaki Y, Kato Y, Sugiyama Y, Kataoka K. Long-circulating poly (ethylene glycol)–poly (d, l-lactide) block copolymer micelles with modulated surface charge. J Control Release. 2001;77(1-2):27-38.

51. Juliano Rá, Stamp D. The effect of particle size and charge on the clearance rates of liposomes and liposome encapsulated drugs. Biochem Biophys Res Commun. 1975;63(3):651-658.

52. Boedtkjer E, Pedersen SF. The acidic tumor microenvironment as a driver of cancer. Annu Rev Physiol. 2020;82:103-126.

53. Shen C, Wang J, Wu X, Xu J, Hu J, Reheman A. Drug release behavior of poly (amino acid) s drug-loaded nanoparticles with pH-responsive behavior. J Drug Deliv Sci Technol. 2023;87:104827.

54. Ting C-W, Chou Y-H, Huang S-Y, Chiang W-H. Indocyanine green-carrying polymeric nanoparticles with acid-triggered detachable PEG coating and drug release for boosting cancer photothermal therapy. Colloids Surf B Biointerfaces. 2021;208:112048.

55. Li X, Liu P. Acid-triggered degradable polyprodrug with drug as unique repeating unit for long-acting drug delivery with minimal leakage. Mater Sci Eng C Mater Biol Appl. 2021;128:112317.

56. Song S, Shen H, Wang Y, Chu X, Xie J, Zhou N, Shen J. Biomedical application of graphene: From drug delivery, tumor therapy, to theranostics. Colloids Surf B Biointerfaces. 2020;185:110596.

57. Lv S, Tang Z, Li M, Lin J, Song W, Liu H, et al. Co-delivery of doxorubicin and paclitaxel by PEG-polypeptide nanovehicle for the treatment of non-small cell lung cancer. Biomaterials. 2014;35(23):6118-6129.

58. Amani A, Begdelo JM, Yaghoubi H, Motallebinia S. Multifunctional magnetic nanoparticles for controlled release of anticancer drug, breast cancer cell targeting, MRI/fluorescence imaging, and anticancer drug delivery. J Drug Deliv Sci Technol. 2019;49:534-546.

59. Montazeri M, Sadeghizadeh M, Pilehvar-Soltanahmadi Y, Zarghami F, Khodi S, Mohaghegh M, et al. Dendrosomal curcumin nanoformulation modulate apoptosis-related genes and protein expression in hepatocarcinoma cell lines. Int J Pharm. 2016;509(1-2):244-254.

60. Ismail NI, Othman I, Abas F, H. Lajis N, Naidu R. Mechanism of apoptosis induced by curcumin in colorectal cancer. Int J Mol Sci. 2019;20(10):2454.

61. Lotfi-Attari J, Pilehvar-Soltanahmadi Y, Dadashpour M, Alipour S, Farajzadeh R, Javidfar S, Zarghami N. Co-delivery of curcumin and chrysin by polymeric nanoparticles inhibit synergistically growth and hTERT gene expression in human colorectal cancer cells. Nutr Cancer. 2017;69(8):1290-1299.

62. Johdi NA, Sukor NF. Colorectal cancer immunotherapy: options and strategies. Front Immunol. 2020;11:1624.

63. Aghabozorgi AS, Sarabi MM, Jafarzadeh-Esfehani R, Koochakkhani S, Hassanzadeh M, Kavousipour S, Eftekhar E. Molecular determinants of response to 5-fluorouracil-based chemotherapy in colorectal cancer: The undisputable role of micro-ribonucleic acids. World J Gastrointest Oncol. 2020;12(9):942.

64. Tecza K, Pamula-Pilat J, Lanuszewska J, Butkiewicz D, Grzybowska E. Pharmacogenetics of toxicity of 5-fluorouracil, doxorubicin and cyclophosphamide chemotherapy in breast cancer patients. Oncotarget. 2018;9(10):9114.

65. Verma H, Narendra G, Raju B, Singh PK, Silakari O. Dihydropyrimidine dehydrogenase-mediated resistance to 5-fluorouracil: Mechanistic investigation and solution. ACS Pharmacol Transl Sci. 2022;5(11):1017-1033.

66. Negrei C, Hudita A, Ginghina O, Galateanu B, Voicu SN, Stan M, et al. Colon cancer cells gene expression signature as response to 5-fluorouracil, oxaliplatin, and folinic acid treatment. Front Pharmacol. 2016;7:172.

67. Puerta-García E, Urbano-Pérez D, Carrasco-Campos MI, Pérez-Ramírez C, Segura-Pérez A, Cañadas-Garre M. Effect

of DPYD, MTHFR, ABCB1, XRCC1, ERCC1 and GSTP1 on chemotherapy related toxicity in colorectal carcinoma. Surg Oncol. 2020;35:388-398.

68. Abbasian MH, Ansarinejad N, Abbasi B, Iravani M, Ramim T, Hamedi F, Ardekani AM. The role of dihydropyrimidine dehydrogenase and thymidylate synthase polymorphisms in fluoropyrimidine-based cancer chemotherapy in an Iranian population. Avicenna J Med Biotechnol. 2020;12(3):157.

69. Cevik M, Namal E, Sener ND, Koksal UI, Cagatay P, Deliorman G, et al. Investigation of DPYD, MTHFR and TYMS polymorphisms on 5-fluorouracil related toxicities in colorectal cancer. J Pers Med. 2022;19(5):435-444.

70. Zheng X, Yang X, Lin J, Song F, Shao Y. Low curcumin concentration enhances the anticancer effect of 5-fluorouracil against colorectal cancer. Phytomedicine. 2021;85:153547.

71. Ni R, Duan D, Li B, Li Z, Li L, Ming Y, et al. Dual-modified PCL-PEG nanoparticles for improved targeting and therapeutic efficacy of docetaxel against colorectal cancer. Pharm Dev Technol. 2021;26(8):910-921.

72. Xiao B, Han MK, Viennois E, Wang L, Zhang M, Si X, Merlin D. Hyaluronic acid-functionalized polymeric nanoparticles for colon cancer-targeted combination chemotherapy. Nanoscale. 2015;7(42):17745-17755.

73. Sadeghi-Abandansari H, Pakian S, Nabid M-R, Ebrahimi M, Rezalotfi A. Local co-delivery of 5-fluorouracil and curcumin using Schiff's base cross-linked injectable hydrogels for colorectal cancer combination therapy. Eur Polym J. 2021;157:110646.

74. Obeng E. Apoptosis (programmed cell death) and its signals-A review. Braz J Biol. 2020;81:1133-1143.

75. Xiang L, He B, Liu Q, Hu D, Liao W, Li R, et al. Antitumor effects of curcumin on the proliferation, migration and apoptosis of human colorectal carcinoma HCT-116 cells. Oncol Rep. 2020;44(5):1997-2008.

76. Szarynska M, Olejniczak A, Wierzbicki P, Kobiela J, Laski D, Sledzinski Z, et al. FasR and FasL in colorectal cancer. Int J Oncol. 2017;51(3):975-986.

77. Çalıbaşı Koçal G, Pakdemirli A, Bayrak S, Ozupek N, Sever T, Başbınar Y, et al. Curcumin effects on cell proliferation, angiogenesis and metastasis in colorectal cancer. J BUON. 2019;24(4).

78. Blondy S, David V, Verdier M, Mathonnet M, Perraud A, Christou N. 5-Fluorouracil resistance mechanisms in colorectal cancer: From classical pathways to promising processes. Cancer Sci. 2020;111(9):3142-3154.

79. Arneth B. Tumor microenvironment. Medicina. 2019;56(1):15.

80. Thakkar S, Sharma D, Kalia K, Tekade RK. Tumor microenvironment targeted nanotherapeutics for cancer therapy and diagnosis: A review. Acta Biomater. 2020;101:43-68.

81. Bhattacharyya S, Md Sakib Hossain D, Mohanty S, Sankar Sen G, Chattopadhyay S, Banerjee S, et al. Curcumin reverses T cell-mediated adaptive immune dysfunctions in tumor-bearing hosts. J Cell Mol Immunol. 2010;7(4):306-315.